Theoretical and Experimental Assessment of Output Performance of Different Configurations of Solar PV Array under Partial Shading Conditions

Niti Agrawal

Associate Professor, Department of Physics, Shyamlal College, University of Delhi, Delhi-110032, India

Abstract— Solar photovoltaic (SPV) has become increasingly popular for generating clean electricity. However, one challenge that affects their performance is partial shading. Partial shading (PS) occurs when certain portions of the solar panel receive reduced solar irradiance due to obstructions such as trees, buildings, dust, snow or debris. The non uniform solar irradiance received by the modules leads to decrease in power generation from the SPV. In the present paper a comprehensive investigation of three different configurations namely Series-Parallel (SP), Bridge Linked (BL) and Total-Cross-Tied (TCT) PV array configurations have been done to find out the configuration least susceptible to the adverse impact of PS. The first half of the present paper undertakes theoretical analysis of the different configurations by writing Kirchhoff's current – voltage equation and solving them using Newton Raphson's method. The second part undertakes experimental investigation of the output performance of different configurations of solar PV array under PS condition using a prototype indoor experiment. Four different shading patterns have been used in this work. The output performance comparison in terms of maximum power delivered, power loss and efficiency among these configurations have been done conducted under different shading patterns.

Keywords— Photovoltaic, Partial Shading, Power loss, Series-Parallel, Bridge Linked, Total-Cross-Tied

DOI: 10.48047/ecb/2023.12.si8.550

1. Introduction

Energy needs of human population across the world have increased rapidly over last few decades. Solar energy has emerged as a crucial renewable energy source, contributing significantly to the global shift towards sustainability [1]. Solar photovoltaic (PV), have become increasingly popular for generating clean electricity [2]. However, one challenge that affects their performance adversely is partial shading [3],[4].

Partial shading is a very common condition which occurs when certain portions of the solar panel receive reduced solar irradiance due to obstructions such as trees, buildings, moving clouds or debris, resulting in huge power loss [5]-[7]. Partial shading can significantly reduce the overall energy production of a solar panel system [8]-[10]. When a part of the panel is shaded, it creates an imbalance in the flow of current. The shaded cells generate less electricity than the unshaded cells, while the unshaded cells continue to operate at current levels higher than those of shaded cells. In a solar PV module, multiple solar cells are generally connected in series, forming a string. Since the current through all the series connected cells must be equal therefore, the shaded cells are forced into reverse bias to conduct the larger current of the unshaded cells. The reverse biased cell acts like a load and starts consuming power instead of generating [11]. This results in mismatch power loss. Also, this could generate excessive heating with a consequent temperature increase in the localized region of shaded cell termed as Hotspot, which can cause the permanent destruction of the encapsulation or cell causing module failure [12],[13].

One way to minimize the power loss due to shading is to add bypass diodes in parallel to the string of solar cells. This not only adds to the cost of the PV systems but also changes the P-V characteristics by introducing multiple local power peaks instead of one global power peak [7],[8]. The other way to reduce the power loss is by implementing different configurations of PV modules in an array. Array configuration refers to the interconnection scheme of the PV cells/modules within the array. Many different types of PV configurations have been investigated by the researchers. Output performance of a partially shaded PV array is dependent not only on the pattern and location of shade but also on its configuration [14]-[17].

In this study performance of three PV array configurations namely Series-Parallel (SP), Bridge-Linked (BL) and Total-Cross-Tied (TCT) under partial shading conditions has been investigated under PSC. In author's previous work a brief examination of different configuration was presented [18]. The present work is a detailed theoretical and experimental investigations conducted on different configurations of a 214 Wp PV array. For the deeper understanding, first theoretical model of each configuration is presented, which is based on: (i) single diode model representing the non-linear current-voltage relation of PV module (ii) Kirchhoff's current and voltage equations for the electrical network of each array configuration (iii) Newton-Raphson method to solve the system of nonlinear equations [19]. The second half of the paper presents the experimental investigations conducted on these configurations under different PSCs using a prototype indoor experiment. Different shadow conditions are used to test the configurations most advantageous in terms of power generation during partial shading. For the comparative analysis maximum power generated, power loss and efficiency are calculated for all the configurations. This study provides the theoretical and experimental guidance for the further research and application. It is beneficial for solar panel system designers and installers who are required to consider shading analysis during the planning phase to optimize PV efficiency.

1.1 Paper Organization

Rest of the paper is organised as follows: Section 2 presents the outline of the methods and procedures used for this study. Section 3 presents the modelling of PV module and different configurations of PV array. Section 4 details about the experimental set up used for this study. Section 5 describes the results and discussion and Section 6 includes the conclusion of the study.

2. Method and Procedure

This section describes the the methods and procedures used in this study, the outline of which is presented in Fig. 1.

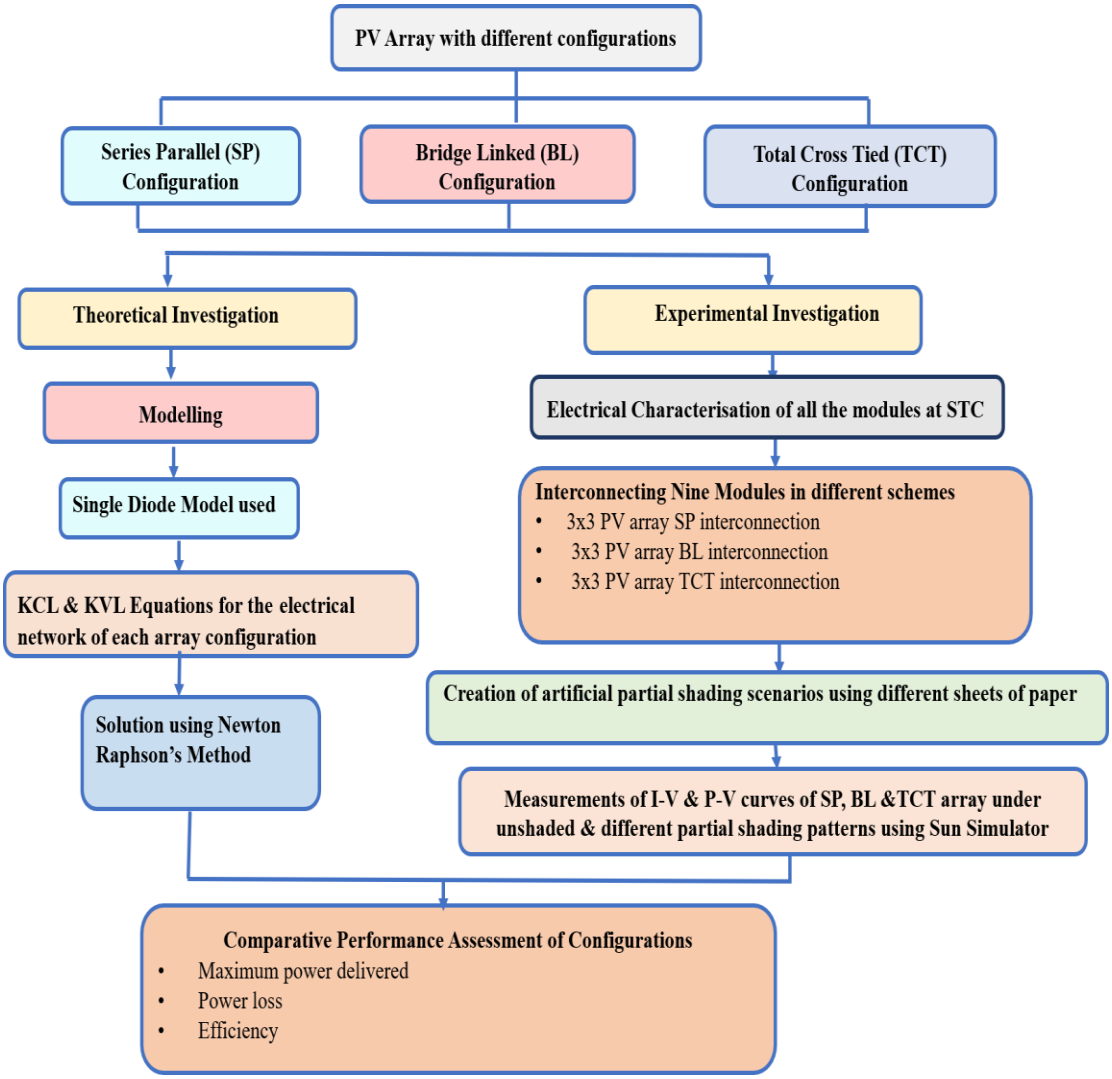

Fig. 1. Outline of Methods and Procedures used in the study.

The details of the methodology used is described in the following sections.

3. Modeling of PV Module

The explicit current-voltage equation for a PV module is given by (1). This equation is based on Single diode model of a solar cell [20],[21].

$$f(I_m, V_m, G) = I_{ph} - I_o\left[\exp\left(\frac{V_m + I_m R_s}{nV_{th}}\right) - 1\right] - \left(\frac{V_m + I_m R_s}{R_{sh}}\right) - I_m = 0 \quad (1)$$

Where I_m and V_m represents the PV module output current and output voltage, I_{ph} is the photogenerated current, Io is the reverse saturation current, R_s and R_{sh} are the PV module series and shunt resistances, n represents the diode ideality factor, $V_{th} = (kTN_s/q)$, is the thermal voltage of the PV module, k is the Boltzmann's constant (1.39×10^{-23}J/K), q is the charge of an electron (1.602×10^{-19} C) and T is the temperature in Kelvin. N_S is the

number of solar cells connected in series in the PV module. The dependence of photo current generated by the module on the solar irradiation (G) and cell temperature (T), is given by (2) [22].

$$I_{ph} = \left[I_{phn} + K_I(T - T_{ref})\right]\left(\frac{G}{G_{ref}}\right) \quad (2)$$

Where I_{phn} is the photo current generated by the module at the standard test conditions (STC), K_I is the current/temperature (A/K) coefficient, T and G are the actual module temperature and solar irradiance respectively. T_{ref} and G_{ref} are the module temperature and solar irradiance at STC (1000 W/m^2 and 25ºC) respectively.

For $T=T_{ref}$, we have from (2)

$$I_{ph} = I_{phn}\frac{G}{G_{ref}} \quad (3)$$

These PV modules are further interconnected to make PV arrays of required capacity. Different configurations of PV array are possible by using different fashion of interconnecting modules.

3.1 Different Configurations of PV Array

Three different configurations considered in this study are explained in this subsection.

1) Series-Parallel (SP) configuration

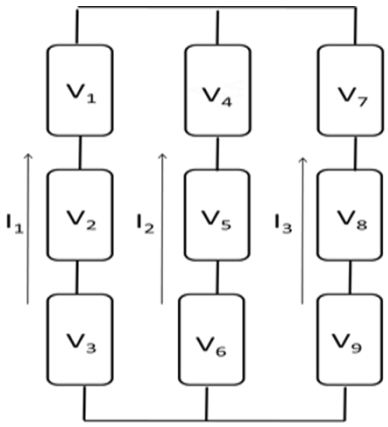

Fig.2. Series-Parallel configuration of 3x3 PV array.

The schematic of a Series-Parallel (SP) configuration is shown in Fig.2. Three modules are first connected in series to form series string and then three such strings are connected in parallel to form a 3x3 SP configured array. The array current (I_a) is the sum of three string currents. The array voltage (V_a) is equal to the voltage of parallel strings. Therefore, following equations are obtained:

$$I_1 + I_2 + I_3 - I_a = 0 \quad (4)$$
$$V_1 + V_2 + V_3 - (V_4 + V_5 + V_6) = 0 \quad (5)$$
$$V_4 + V_5 + V_6 - (V_7 + V_8 + V_9) = 0 \quad (6)$$

Also eq. (7) represents 09 different I-V equations for nine modules of the 3x3 SP configured array by using their individual current and voltage (as indicated in Fig.2).

$$f(I_k, V_i, G_i) = I_{phi} - I_{oi}\left[\exp\left(\frac{V_i + I_k R_{si}}{n_i V_{th}}\right) - 1\right] - \left(\frac{V_i + I_k R_{si}}{R_{shi}}\right) - I_k = 0 \quad (7)$$

$$i = \begin{cases} 1,2,3 \text{ for } k = 1 \\ 4,5,6 \text{ for } k = 2 \\ 7,8,9 \text{ for } k = 3 \end{cases}$$

Equation (4)-(7) are used to find the 12 unknown variables (03 currents and 09 voltages) of 3x3 SP array.

2) Bridge-Linked (BL) configuration

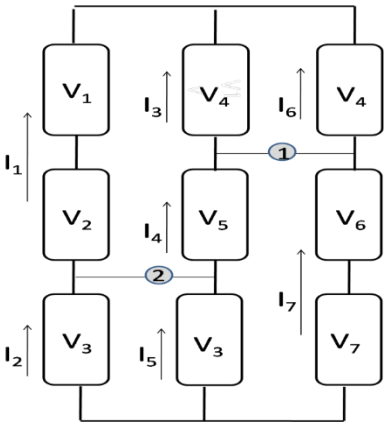

Fig.3. Bridge-Linked configuration of 3x3 PV array.

The schematic of a Bridge-Linked (BL) configuration is shown in Fig.3. It is obtained by interconnecting PV modules in bridge rectifier pattern. Two modules are connected in series which in turn is connected in parallel with other two series connected modules. There are 14 unknowns in the circuit (07 currents and 07 voltages). Applying Kirchhoff's current and voltage equations at node 1 and node 2, following equations are obtained:

$$I_1 + I_4 - I_2 - I_5 = 0 \quad (8)$$
$$I_4 + I_7 - I_3 - I_6 = 0 \quad (9)$$
$$V_1 + V_2 - V_4 - V_5 = 0 \quad (10)$$
$$V_3 + V_5 - V_6 - V_7 = 0 \quad (11)$$
$$V_1 + V_2 + V_3 - V_a = 0 \quad (12)$$

Eq. (13) represents 09 different I-V equations for nine modules of a 3x3 BL configured array are obtained by using their individual current and voltage (as indicated in Fig.3).

$$f(I_k, V_i, G_i) = I_{phi} - I_{oi}\left[\exp\left(\frac{V_i + I_k R_{si}}{n_i V_{th}}\right) - 1\right] - \left(\frac{V_i + I_k R_{si}}{R_{shi}}\right) - I_k = 0 \quad (13)$$

$$i = \begin{cases} 1,2 \text{ for } k = 1 \\ k+1 \text{ for } k = 2,3,4 \\ k-2 \text{ for } k = 5,6 \\ 6,7 \text{ for } k = 7 \end{cases}$$

Equation (8)-(13) are used to find the 14 unknown variables (07 currents and 07 voltages) of 3x3 BL array.

3) Total-Cross-Tied (TCT) configuration

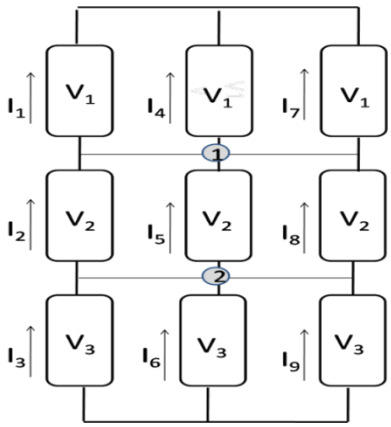

Fig.4 Total-Cross-Tied configuration of 3x3 PV array

The schematic of a Total-Cross-Tied (TCT) configuration is shown in Fig.4. It is obtained by connecting ties across each row of junction. All three modules in each row are connected in parallel and there are three such rows connected in series. Array current is equivalent to any row current. Array voltage is equal to the sum of voltages across each row. Applying Kirchhoff's current and voltage equations at node 1 and node 2, following equations are obtained:

$$I_1 + I_4 + I_7 - I_2 - I_5 - I_8 = 0 \quad (14)$$
$$I_2 + I_5 + I_8 - I_3 - I_6 - I_9 = 0 \quad (15)$$
$$V_1 + V_2 + V_3 - V_a = 0 \quad (16)$$

equation (17), 09 different I-V equations for nine modules of a 3x3 TCT configured array are obtained by using their individual current and voltage (as indicated in Fig.4).

$$f(I_k, V_i, G_i) = I_{phi} - I_{oi}\left[\exp\left(\frac{V_i + I_k R_{si}}{n_i V_{th}}\right) - 1\right] - \left(\frac{V_i + I_k R_{si}}{R_{shi}}\right) - I_k = 0 \quad (17)$$

$$i = \begin{cases} 1 \text{ for } k = 1,2,3 \\ 2 \text{ for } k = 4,5,6 \\ 3 \text{ for } k = 7,8,9 \end{cases}$$

Equation (14)-(17) are used to find the 12 unknown variables (09 currents and 03

voltages) of 3x3 TCT array.

The value of G used for individual modules is as per the shading pattern (explained in sec. 4.4). The value of five parameters (I_o, I_{ph}, n, R_s, R_{sh}) for each module is determined using the method given in [23]. These non-linear equations are simultaneously solved using Newton Raphson's method to get the output characteristics of the configurations.

It is important to mention here that while constructing an array, all identical modules in terms of electrical parameters are used, yet there is always some mismatching within the PV array. However, this aspect has been ignored in previous theoretical work where the electrical characteristics of all the modules constituting the PV array have been assumed to be identical under standard test conditions. In the present analysis, keeping in mind the realistic scenario, the individual electrical parameters of all the PV modules are used in the theoretical modelling.

4. Experimental Set Up

4.1 PV Modules and interconnections

For this work nine multi crystalline Si modules of name plate rating 23Wp, (each having 36 cells in series) arranged in a 3x3 sized array has been used. For the investigations, while keeping the nine PV modules same, their interconnections have been changed to form the SP, BL and TCT configurations of array, as presented in Fig. 5. a-5. c.

4.2 Instrument Used for the I-V measurement

The output current-voltage and power-voltage characteristics of the modules and arrays are measured using a sun simulator namely Gsola XJCM-9A 2006 model is used (Fig.5.d). It is certified to IEC60904-9 class A (AM 1.5 spectral distribution) simulator. The spectral match, temporal stability and non-uniformity of irradiance is as per ASTM E-927/IEC60904-9 AAA class standard. Xenon lamps are used to simulate sun light and produce light whose wavelength ranges from 400nm to 1100nm. The modules are faced down and light irradiates the modules below it.

4.3 Electrical Characterization of PV Modules

The output characteristics of nine PV modules were recorded at the Standard Test Conditions (STC) of 1000 W/m^2 and 25°C. Table 1. displays the values of open circuit voltage (V_{OC}), short circuit current (I_{SC}), voltage at maximum power (V_M) and current at maximum power (I_M) of independent modules. Though the name plate rating of these modules is same (23 Wp), however a slight mismatch in terms of the electrical parameters resulting in minor variation in their maximum output power is observed.

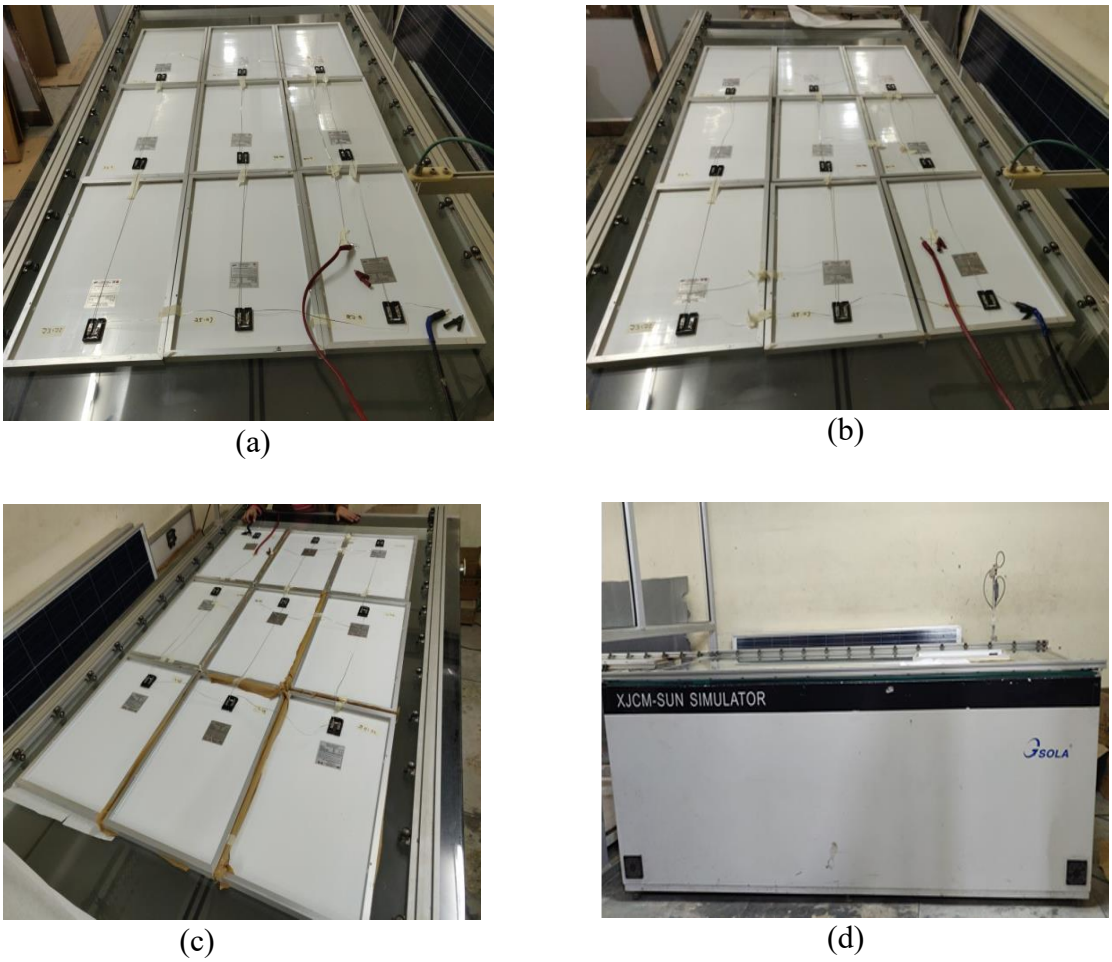

Fig.5 Experimental Set up (a) 3x3 SP Configuration (b) 3x3 BL Configuration (c) 3x3 TCT configuration (d) Sun Simulator used

Table 1. Electrical parameters of the nine PV modules used in 3x3 PV array.

PV module No.	**V_{oc} (V)**	**I_{sc} (A)**	**V_m (V)**	**I_m (A)**
1	22.33	1.45	18.51	1.36
2	22.36	1.36	18.62	1.27
3	22.34	1.32	18.86	1.21
4	22.33	1.37	18.56	1.26
5	22.52	1.43	18.60	1.33
6	22.63	1.39	18.47	1.29
7	22.45	1.39	18.48	1.29
8	22.46	1.44	18.74	1.34
9	22.20	1.32	18.53	1.25

4.4 Creation of Different Partial Shading Conditions

For this work, shading cases which differ in terms of shape, size and shade intensity are created artificially by masking some of the modules of the array by three sheets of different transmissivity.

For $T=T_{ref}$ (Temperature in a solar simulator is maintained at 25ºC (STC)) and $I_{ph} \approx I_{sc}$, we have form Eq. (2)

$$\frac{I_{sc}}{I_{scn}} = \frac{G}{G_{ref}} \tag{18}$$

The above equation has been used to find the value of transmittivity of different sheets and hence the shading intensity created by them on the module. A reference module was masked by different sheets one by one and change in the value of short circuit current (I_{sc}) with respect to its value at G_{ref}=1000 W/m^2 (I_{scn}) was observed. Using eq (18) the values transmissivity of sheets and hence their shading strength are estimated and is given in Table 2.

Table 2. Ttransmissivity and shading strength of the sheets used to create partial shading conditions.

Sheet	**Transmittivity (%)**	**Approx. Shading (%)**
Sheet-1	45.6	55
Sheet-2	27.9	72
Sheet-3	10.1	90

Four distinct shading patterns used are named as case-A (uneven column shading), case-B (uneven row shading), case-C (square shaped uneven shading) and case-D (diagonal uneven shading).and is illustrated in Fig. 6.

4.5 Comparative Output Performance Assessment of PV array configurations

4.5.1 Partial Shading Power Loss

Partial Shading Power Loss (ΔP_{PSPL}) is the difference between the maximum obtained power from the array without any shading ($P_{max,un}$) and maximum power obtained from the array under partial shading condition ($P_{max,sh}$)

$$\Delta P_{PSPL} = P_{max,un} - P_{max,sh} \tag{19}$$

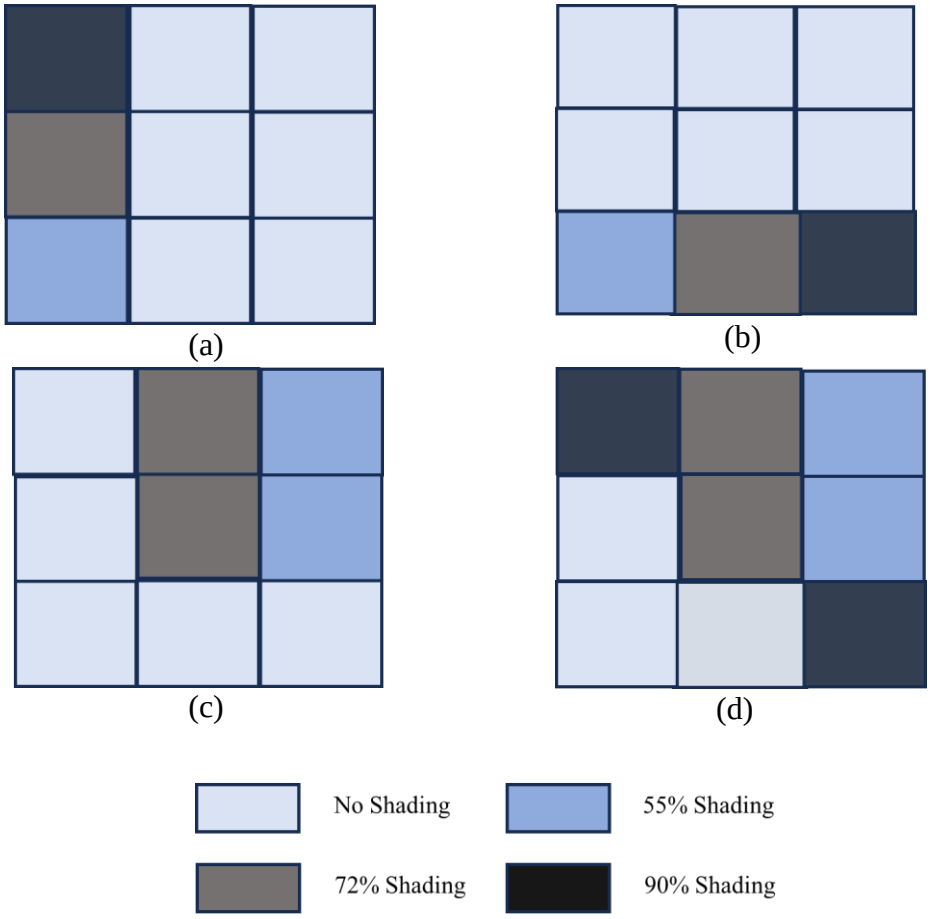

Fig. 6. Shading patterns used on 3x3 PV array (a) case-A (uneven column shading), (b) case-B (uneven row shading), (c) case-C (square shaped uneven shading), (d) case-D (diagonal uneven shading)

4.5.2 Efficiency

Efficiency (η) is defined as the ratio of the maximum output power generated by the PV array to the input power from sun.

$$\eta\ (\%) = \frac{\mathrm{P_{out}}}{P_{in}} \times 100 \qquad (20)$$

Where, P_{in}=G x A, 'G' is the input solar irradiance per unit area (W/m^2) and 'A' is the area of the PV array on which it falls.

5. Result and Discussion

5.1 Output power of different array configurations at uniform irradiance

Under uniform irradiance of 1000 W/m^2 and temperature of 25ºC, P-V characteristics of SP, BL, TCT configuration is represented in Fig 7. As is evident from the curve all configurations provide same output power of 207 W.

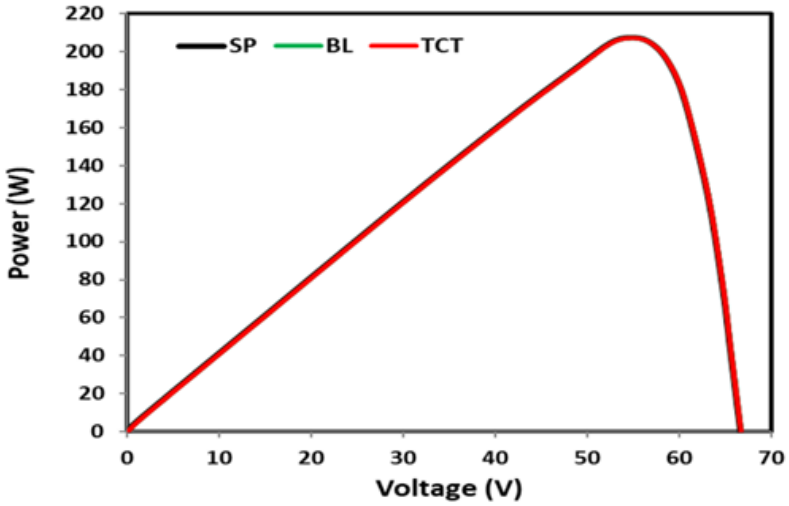

Fig. 7 P-V characteristics of 3x3 SPV array at STC

However, the sum of maximum power of all modules at 1000 W/m^2 and 25ºC adds to 214.2 W (same as theoretically obtained maximum power). The mismatching of electrical parameters and wiring loss results in an approximately 3.3 % power loss even when there is no shading. When subjected to partial shading conditions, the output performance of these configurations becomes different from each other.

5.2 Output power of different array configurations under different partial shading cases

Case-A: In this case one column of 3x3 SPV array was non-uniformly shaded.

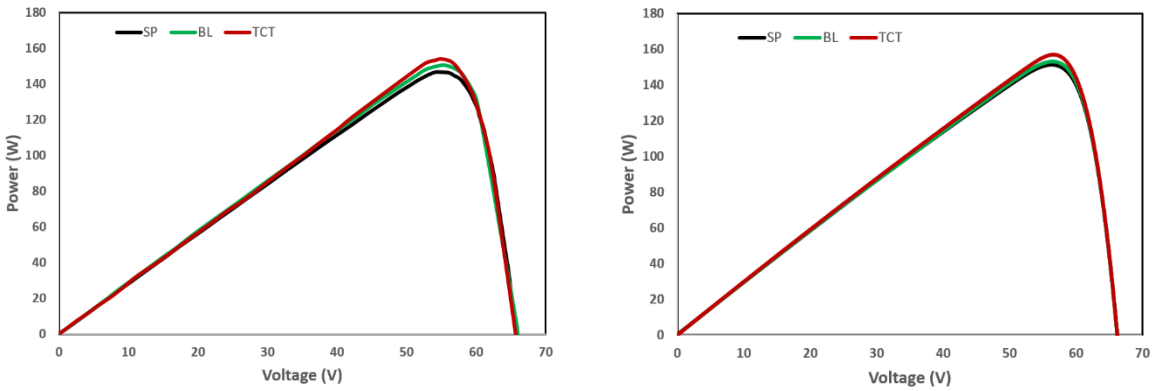

Fig. 8 (a) Experimentally and (b) Analytically obtained P-V characteristics of 3 x3 SPV array under shading case-A (uneven column shading).

Experimentally and analytically obtained P-V characteristics of all the configurations under this condition is represented in Fig 8 (a) and (b) respectively. It is found form experimental results that maximum output power is generated by TCT (153.8 W) while

BL and SP generates lesser power of 150.1 W and 147.6 W respectively.

Case-B: In this case one row of 3x3 SPV array was non-uniformly shaded. Experimentally and analytically obtained P-V characteristics of all the configurations under this condition is represented in Fig. 9 (a) and (b) respectively.

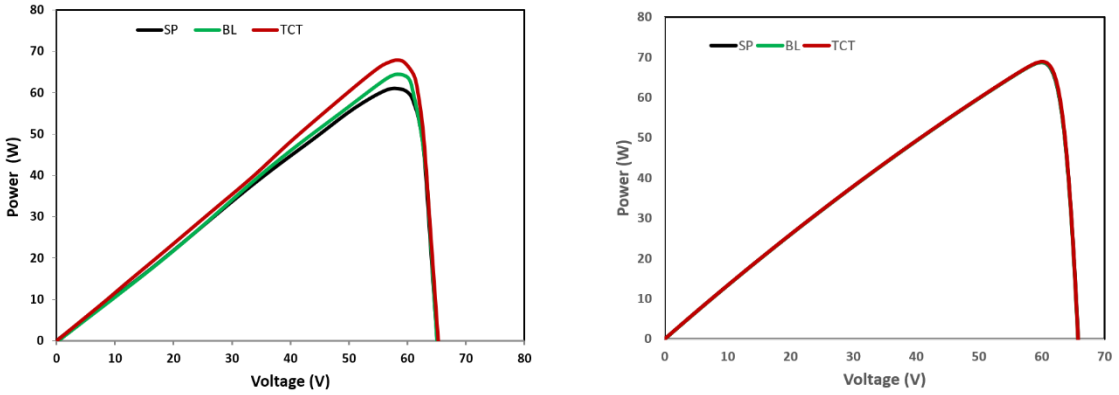

(a) (b)

Fig. 9 (a) Experimentally and (b) Analytically obtained P-V characteristics of 3x3 SPV array under shading case-B (uneven row shading).

It is observed that under this shading scenario, output performance of all the configurations has deteriorated, with TCT still generating maximum power of 67.9 W followed by BL generating 64.5 W and SP 61.2 W.

Case-C: In this case, two modules of second column has solar irradiance of 456 W/m^2, two adjacent modules of third column has solar irradiance of 279 W/m^2 with remaining five modules at 1000 W/m^2 forming a non-uniform square shading.

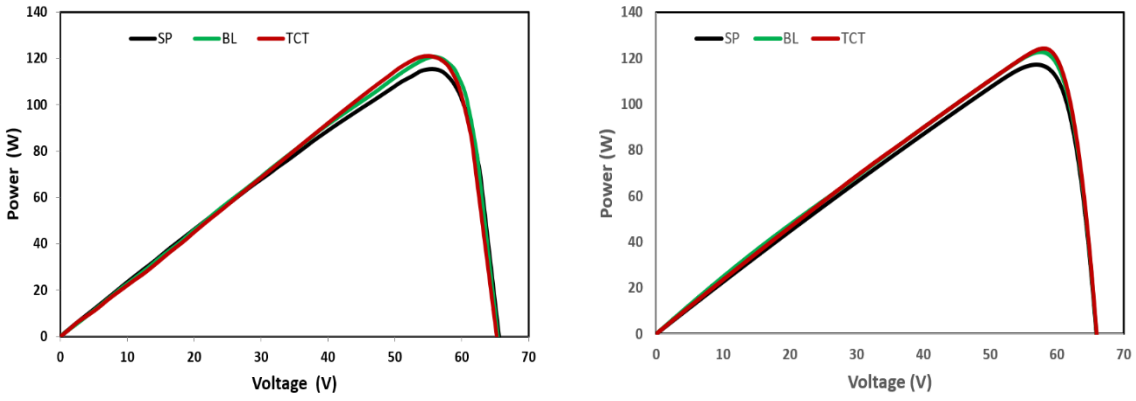

(a) (b)

Fig. 10 (a) Experimentally and (b) Analytically obtained P-V characteristics of 3x3 SPV array under shading case-C (uneven square shading).

Experimentally and analytically obtained P-V characteristics of all the configurations under this condition is represented in Fig.10 (a) and (b) respectively. It is observed that TCT and BL provide nearly same power (120.7 W and 120.3 W respectively). SP generates minimum power of 115.0 W.

Case-D: In this case 3x3 SPV array was diagonally shaded with non-uniform irradiance. Experimentally and analytically obtained P-V characteristics of all the configurations under this condition is represented in Fig. 11 (a) and (b) respectively. As found from the results, power generation of all the configurations is reduced drastically under this shading scenario. SP generates only 34.0 W while BL generate 44.0 W. TCT generates the maximum power of 63.9 W.

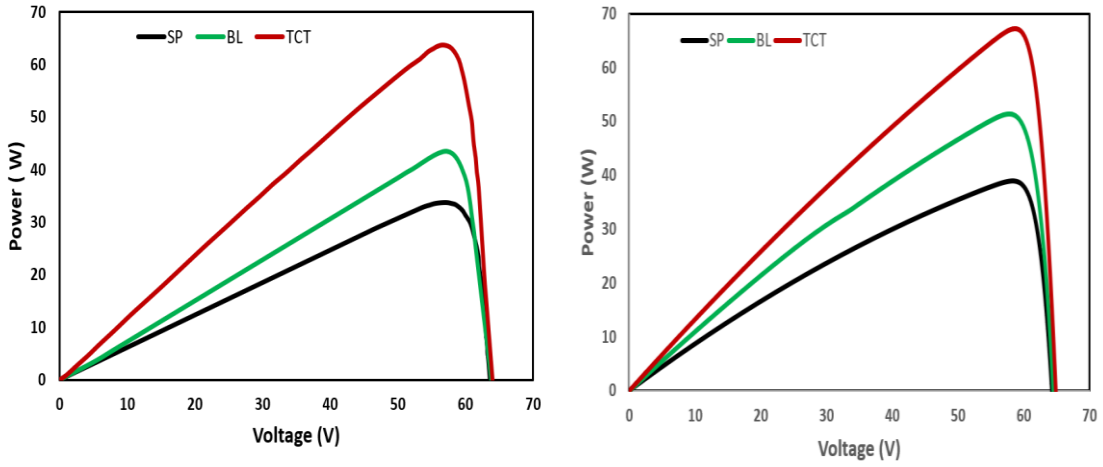

(a) (b)

Fig. 11 (a) Experimentally and (b) Analytically obtained P-V characteristics of 3x3 SPV array under shading case-D (uneven diagonal shading).

Table 3. represents the experimental and theoretical values of maximum power generated by different configurations under different partial shading conditions. The small difference in the experimental and theoretical values is due to slight mismatching of electrical parameters of PV modules and due to power loss in wiring. Third column of the table represents the power enhancement (%) achieved by changing the fashion of interconnections of modules from SP to BL and TCT respectively. Though power is enhanced for all the shading cases, maximum increase in power is obtained for case-D.

Table 3. Comparison of Power Generated by SP, BL and TCT configuration of 3x3 PV array under different Partial Shading conditions

Shading Case	Experimental Maximum Power in (W)			Theoretical Maximum Power in (W)			Power Enhancement (%)		
	SP	**BL**	**TCT**	**SP**	**BL**	**T CT**	**SP**	**BL**	**TCT**
Case-A	147.6	150.1	153.8	151.2	153.3	157.1	-	1.2	3.0
Case-B	61.2	64.5	67.9	67.4	68.2	68.9	-	1.6	3.3
Case-C	115.0	120.3	120.7	117.2	122.7	124.3	-	2.7	2.8
Case-D	34.0	44.0	63.9	36.5	51.0	67.2	-	5.1	14.4

5.3 Comparative Partial Shading Power Loss in PV array configurations

The power loss suffered by SP, BL and TCT array under all the partial shading conditions is represented in Fig 12. It is evident that power loss due to shading depends greatly on the shading pattern. Obtained power loss is minimum for case A and maximum for case D for all the configurations. However, under all shading patterns TCT configuration displays least power loss followed by BL PV array configuration.

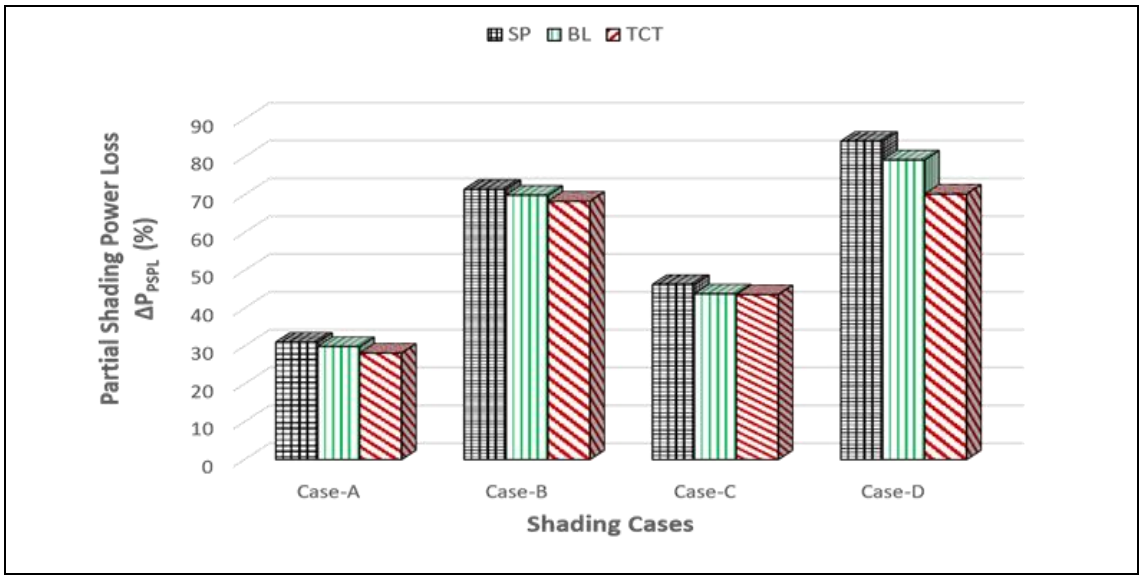

Fig 12. Power loss suffered by SP, BL and TCT array under different partial shading cases.

5.4 Comparative Efficiencies of PV array configurations

The efficiencies of SP, BL and TCT array under all the partial shading conditions have been calculated using (11) and represented in Fig 13. For case B, efficiency increase from 3.0 % to 4.9 % by changing interconnection from SP to TCT. Under shading pattern D, efficiency nearly doubles, from 3.5 % to 6.6 %, by changing interconnection from SP to TCT. In general TCT PV configurations has shown maximum efficiency under all considered shading patterns.

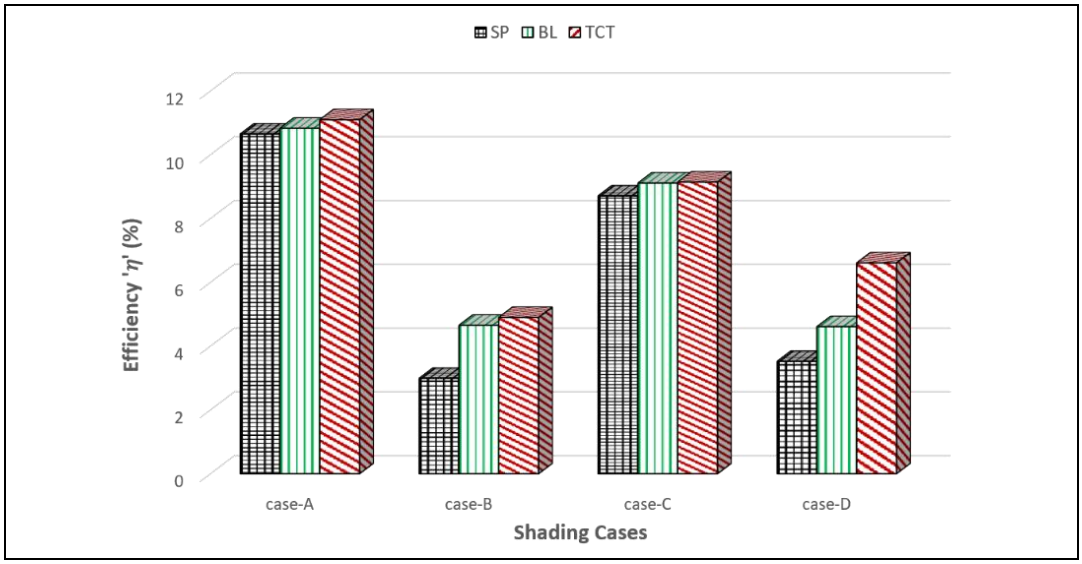

Fig 13. Efficiency of SP, BL and TCT array under different partial shading cases.

6. Conclusion

In this work impact of partial shading on a 3x3 SPV array in SP, BL and TCT configuration has been reviewed theoretically as well as experimentally. Four different shading conditions were created for this investigation. The P-V curves for all the configurations under different partial shading conditions have been plotted. The experimentally obtained results are validated using mathematical model of the PV array. The power loss of a solar PV array under partial shading conditions depends on the shading pattern, intensity and its configuration. Power loss and efficiency for all the configurations for all shading cases have been calculated. Under all shading cases TCT generates maximum power and has maximum efficiency, followed by BL configuration. SP configuration is most susceptible to power loss when partially shaded. This study conclusively establishes that TCT configuration is the optimum configuration which can enhance power generation and minimize power loss under partial shading conditions.

This study provides the theoretical and experimental guidance for the further research and application. It is beneficial for solar panel system designers and installers who are required to consider shading analysis during the planning phase to optimize PV efficiency.

References

[1] "REN 21: Renewables 2021 Global Status Report," 2021.

[2] "Future of solar photovoltaic: Deployment, investment, technology, grid integration and socio-economic aspects," IRENA, November 2019.

[3] M. Aghaei et al., "Review of degradation and failure phenomena in photovoltaic modules," Renewable and Sustainable Energy Reviews, vol. 159, p. 112160, May 2022, doi: 10.1016/J.RSER.2022.112160.

[4] N.D. Kaushika and A.K. Rai, "An investigation of mismatch losses in solar photovoltaic cell networks," Energy, vol.32, pp 755–759, 2007.

[5] K. Lappalaine and S. Valkealahti, "Photovoltaic mismatch losses caused by moving clouds," Solar Energy, vol. 158, pp 455-461, 2017.

[6] M.R.Maghami, H Hizam, C Gomes, M Amran Radzi , Mohammad Ismael Rezadad , Shahrooz Hajighorbani, " Power loss due to soiling on solar panel: A review," Renewable and Sustainable Energy Reviews, vol. 59, pp 1307–1316, 2016.

[7] S.R. Pendem and S. Mikkili, "Modelling and performance assessment of PV array configurations under partial shading conditions to mitigate the mismatching power losses". Solar Energy, vol. 160, pp 303-321, 2018.

[8] Sara Gallardo-Saavedra and Björn Karlsson, "Simulation, validation and analysis of shading effects on a PV system," Solar Energy, vol.170, pp 828-839, 2018.

[9] F. Salem and M.A. Awadallah, "Detection and assessment of partial shading in photovoltaic arrays," Journal of Electrical Systems and Information Technology, vol 3(1), pp 23-32, 2016.

[10] H. Patel and V. Agarwal, "MATLAB based modelling to study the effects of partial shading on PV array characteristics," IEEE Trans. on Energy Conversion, vol. 23 (1), pp 302-310, 2008.

[11] J. W. Bishop, "Computer simulation of the effects of electrical mismatches in photovoltaic cell interconnection circuits," Solar Cells, vol. 25, no. 1, pp. 73–89, Oct. 1988, doi: 10.1016/0379-6787(88)90059-2.

[12] S. M. Shrestha et al., "Determination of Dominant Failure Modes Using FMECA on the Field Deployed c-Si Modules Under Hot-Dry Desert Climate," IEEE Journal of Photovoltaics, vol. 5, no. 1, pp. 174–182, 2015, doi: 10.1109/JPHOTOV.2014.2366872.

[13] D. C. Jordan, T. J. Silverman, J. H. Wohlgemuth, S. R. Kurtz, and K. T. VanSant, "Photovoltaic failure and degradation modes," Progress in Photovoltaics: Research and Applications, vol. 25, no. 4, pp. 318–326, 2017, doi: https://doi.org/10.1002/pip.2866.

[14] Okan Bingöl and Burcin Özkaya, "Analysis and comparison of different PV array configurations under partial shading conditions," Solar Energy, vol. 160, pp 336-343, 2018.

[15] R. Pachauri, R. Singh, A. Gehlot, R. Samakaria, S. Choudhury, "Experimental analysis to extract maximum power from PV array reconfiguration under partial shading conditions" Engineering Science and Technology, an International Journal, vol. 22, pp 109–130,2019.

[16] S. Pareek, N. Chaturvedi and R. Dahiya, "Optimal interconnections to address partial shading losses in solar photovoltaic arrays". Solar Energy, vol. 155, pp 537–551, 2017.

[17] N. Argawal and A. Kapoor, "Investigation of the effect of partial shading on series and parallel connected solar photovoltaic modules using Lambert W-function", 2018. AIP Conf. Proc.2006,030050-1-030050-5.

[18] Niti Agrawal and Avinashi Kapoor, "Power loss mitigation in partially shaded solar PV array through different interconnection configurations," AIP Conference Proceedings 2136, 040012 (2019); https://doi.org/10.1063/1.5120926

[19] Y.J Hsu and P.C. Hsu, "An investigation on partial shading of PV modules with different connection configurations of PV cells," Energy, vol. 36, pp 3069–3078, 2011.

[20] M. G. Villalva, J. R. Gazoli, and E. R. Filho, "Comprehensive approach to modeling and simulation of photovoltaic arrays," IEEE Trans Power Electron, vol. 24, no. 5, pp. 1198–1208, 2009, doi: 10.1109/TPEL.2009.2013862.

[21] M. Kermadi, V. J. Chin, S. Mekhilef, and Z. Salam, "A fast and accurate generalized analytical approach for PV arrays modeling under partial shading conditions," Solar Energy, vol. 208, pp. 753–765, Sep. 2020, doi: 10.1016/J.SOLENER.2020.07.077.

[22] M.G. Villalva, "Comprehensive approach to modelling and simulation of photovoltaic arrays," IEEE Trans. Power Electron., vol. 24, pp 1198-1208, 2009.

[23] J.Cubas, S. Pindado and Carlos de Manuel, " Explicit expression for solar panel equivalent circuit parameters based on analytical formulation and the Lambert W-function" Energies, vol. 7, pp 4098–4115, 2014.